

Published in final edited form as:

J Neurochem. 2008 November ; 107(4): 987–1000. doi:10.1111/j.1471-4159.2008.05659.x.

Mechanisms for Recycling and Biosynthesis of Endogenous Cannabinoids Anandamide and 2-Arachidonylglycerol

Ekaterina A. Placzek¹, Yasuo Okamoto², Natsuo Ueda², and Eric L. Barker¹

¹ Department of Medicinal Chemistry and Molecular Pharmacology, Purdue University, 575 Stadium Mall Drive, West Lafayette, IN 47904

² Department of Biochemistry, Kagawa University School of Medicine, 1750-1 Ikenobe, Miki, Kagawa 761-0793, Japan

Abstract

The mechanisms of endogenous cannabinoid biosynthesis are not completely understood. We hypothesized that anandamide could be recycled by the cell to form new endocannabinoid molecules and released into the extracellular space. We determined that new endocannabinoids derived from exogenous anandamide or arachidonic acid were synthesized and released from RBL-2H3 cells in response to ionomycin. Treatment of RBL-2H3 cells with nystatin and progesterone, agents that disrupt organization of lipid raft/caveolae, resulted in the attenuation of anandamide and 2-arachidonyl glycerol synthesis and/or release in response to stimulation with ionomycin suggesting a role for these membrane microdomains in endocannabinoid biosynthesis. Furthermore, anandamide synthesis may be independent of *N*-acyl phosphatidylethanolamine phospholipase D as expression of the enzyme was not detected in RBL-2H3 cells. We also established that extracellular calcium is necessary for endocannabinoid biosynthesis because release of intracellular calcium stores alone does not promote endocannabinoid biosynthesis. Next, we examined the role of calcium as a “switch” to activate the synthesis of anandamide and simultaneously reduce uptake. Indeed, [³H] anandamide uptake was reduced in the presence of calcium. Our findings suggest a mechanism indicative of calcium-modulated activation of anandamide synthesis and simultaneous termination of uptake.

Keywords

anandamide; 2-arachidonoyl glycerol; arachidonic acid; membrane microdomains; caveolae

Introduction

Delta-9-tetrahydrocannabinol (Δ^9 -THC) is the primary psychoactive component of marijuana, a naturally occurring plant-derived cannabinoid (Childers and Breivogel, 1998). Δ^9 -THC produces a wide range of pharmacological effects both in the central nervous system and in the periphery. Δ^9 -THC elicits therapeutic benefits when used for treatment of glaucoma, spasticity, and pain, however, the beneficial effects of Δ^9 -THC are hampered by the psychotropic side effects (Watson et al., 2000). The undesirable side effects elicited by Δ^9 -THC include alterations in cognition and memory as well as the feeling of a “high” or euphoria.

The endogenous cannabinoids (endocannabinoids) anandamide (AEA) and 2-arachidonyl glycerol (2-AG) mimic the actions of Δ^9 -THC, as the pharmacologic profiles of endogenous and plant-derived cannabinoids are similar. AEA, 2AG, as well as Δ^9 -THC mediate their effects primarily via the G protein-coupled CB1 and CB2 cannabinoid receptors (Matsuda et al., 1990; Munro et al., 1993). AEA has also been shown to be an agonist at the vanilloid receptor (VR1) that is a member of the transient receptor potential (TRP) superfamily of ion channels (Smart et al., 2000; Zygmunt et al., 1999). Both AEA and 2-AG have been linked to retrograde signaling in various brain regions (Chevalleyre et al., 2006). Furthermore, endocannabinoids modulate many diverse biological targets, and therefore play a role in physiological processes such as pain, nausea, reproduction, immune response, and cancer (Di Carlo and Izzo, 2003; Guzmán, 2003; Habayeb et al., 2002; Karsak et al., 2007; Parolaro et al., 2002; Pertwee, 2001; Tramèr et al., 2001). Characterization and pharmacologic manipulation of the endocannabinoid system is important because it may allow us to identify new drug targets for the treatment of many disorders without the undesirable psychotropic side effects that plant-derived cannabinoids produce.

The pharmacologic profiles of 2-AG and AEA are similar, including the events that lead to the signal termination of these endocannabinoids (Lambert and Fowler, 2005). To terminate the signaling of 2-AG and AEA, these molecules have to be taken up by the cell. Our lab has previously shown that AEA uptake is an endocytic process that is non-clathrin-mediated, rapid, saturable, and temperature-dependent (McFarland et al., 2008; McFarland et al., 2004). The identity of the protein(s) involved in the transport of both 2-AG and AEA, however, is not known. Following uptake, 2-AG may be hydrolyzed either by fatty acid amide hydrolase (FAAH) or monoacylglycerol lipase to yield ARA and glycerol, whereas AEA is hydrolyzed by FAAH into ARA and ethanolamine (Cravatt and Lichtman, 2003; Deutsch and Chin, 1993; Di Marzo, 1998; Di Marzo et al., 1998; Goparaju et al., 1998).

Our lab has also previously discovered that AEA metabolites, ARA and ethanolamine, are trafficked back to the plasma membrane accumulating in the caveolin-rich membranes, i.e. lipid rafts (McFarland et al., 2004). Lipid rafts are specialized microdomains in the plasma membrane that are enriched in ARA, cholesterol, plasmenylethanolamine, and sphingolipids (London and Brown, 2000; Pike et al., 2002). Caveolae are flask-shaped invaginations of the plasma membrane that are a subclass of lipid rafts (Razani et al., 2002).

Endocannabinoids are synthesized and released in a calcium-dependent fashion “on demand,” unlike the typical neurotransmitter molecules that are stored in and recycled into vesicles. 2-AG and AEA as well as their congeners are thought to be stored in the membrane as phospholipid precursors (Piomelli, 2003). The endocannabinoid 2-AG is synthesized from diacylglycerol via the actions of sn1-specific diacylglycerol lipase in a calcium-dependent fashion (Bisogno et al., 2003). Studies suggest that one of the prevailing pathways for AEA synthesis involves the calcium-dependent enzyme, NAPE PLD. In 2004, Okamoto and colleagues cloned a phospholipase D that specifically synthesized *N*-acylethanolamines (NAEs), including AEA (Okamoto et al., 2004). The role of NAPE PLD in AEA biosynthesis remains unclear because in a separate study, Leung and colleagues reported that the levels of AEA and its precursor were unchanged in the brains of NAPE PLD knock-out mice (Leung et al., 2006). Therefore, purified NAPE PLD may be able to catalyze the formation of AEA *in vitro*, however, other biosynthetic pathways may control the formation of this endocannabinoid *in vivo*.

The present study reveals that the synthesis of AEA and 2-AG depends on the intact organization of lipid raft microdomains in rat basophilic leukemia RBL-2H3 cells. The disruption of lipid rafts with nystatin/progesterone treatment (McFarland et al., 2004; Rothberg et al., 1992; Smart et al., 1996) results in the attenuation of AEA and 2-AG

formation. These results imply that AEA and 2-AG formation and release may take place in the lipid raft/caveolae microdomains of the cell membrane. Furthermore, our findings reinforce the hypothesis that AEA metabolites can be recycled to form new AEA molecules. In addition to recycling AEA into new AEA molecules, RBL-2H3 cells also recycle AEA-derived ARA into 2-AG. In fact, Rimmerman and colleagues established that the biochemical machinery for the production of 2-AG is localized within lipid rafts suggesting that 2-AG synthesis via diacylglycerol occurs within these microdomains (Rimmerman et al., 2008).

The biosynthesis of endocannabinoids is a calcium-dependent process. Therefore, we explored the role of the source of calcium in the synthesis of AEA and 2-AG in RBL-2H3 cells. We removed calcium from the extracellular space and stimulated RBL-2H3 cells with thapsigargin to trigger the release of intracellular calcium stores. We discovered that the biosynthesis of AEA and 2-AG is strictly dependent of the presence of extracellular calcium.

We previously reported that AEA uptake takes place via a caveolae-related endocytosis (McFarland et al., 2008; McFarland et al., 2004), thus, suggesting that both uptake and release of AEA occur from the same microdomain within the plasma membrane. Therefore, we examined whether the cell may utilize calcium as a “switch” by which synthesis and release is activated and the uptake process is disengaged.

Materials and Methods

Cell Culture

RBL-2H3 and HEK-293 cells were maintained in Dulbecco's modified Eagle's medium (DMEM) with 5% fetal clone I and 5% bovine calf serum supplemented with 2 mM L-glutamine and 1% penicillin/streptomycin. CAD cells were maintained in DMEM/F-12 (50/50) with 5% fetal clone I and 5% bovine calf serum supplemented with 2 mM L-glutamine and 1% penicillin/streptomycin. Cells were maintained in a CO₂-containing (5%) humidified environment at 37 °C.

[³H] ARA or [³H] AEA Recycling and Synthesis in RBL-2H3 Cells

RBL-2H3 cells were plated at 3×10^5 cells/well seeding density in 6-well culture plates. Twenty four hours after plating, 1 nM [³H] ARA (American Radiolabeled Chemicals Inc.) or 1 nM [³H] AEA (Perkin Elmer) was added to the cells. The tritiated species were allowed to metabolize and become incorporated into the membrane for the next 24 hours at 37 °C. For the assay, cells were washed twice with Krebs-Ringer Hepes (KRH) buffer (120 mM NaCl, 4.7 mM KCl, 1.2 mM KH₂PO₄, 1.2 mM MgSO₄, 10 mM Hepes and 2.2 mM CaCl₂, pH 7.1) at 37 °C with 0.5% fatty-acid free Bovine Serum Albumin (BSA) and once with KRH buffer without BSA. For the assays examining the role of lipid rafts in the endocannabinoid synthesis, cells were incubated in KRH buffer containing nystatin (25 µg/mL)/progesterone (10 µg/mL) or KRH buffer without nystatin and progesterone for 30 min at 37 °C. One of the indicated treatment conditions included a 100 µM AM404 treatment. Cells were then treated with either KRH buffer or 1 µM ionomycin (Sigma) for 10 min at 37 °C in order to stimulate endocannabinoid synthesis. The reaction buffer was then collected and mixed with ice-cold 1.5 mL of 2:1 chloroform:methanol (vol:vol) and 10 µL of 1 M HCl. The aqueous and organic phases were mixed by vortexing and then separated by centrifugation (2000 × g, 10 min, 4 °C). The organic layer was removed from each sample, placed in a clean glass tube, and 1 mL of ice-cold chloroform was added to the remaining aqueous layer. The phases were again mixed by vortexing and separated by centrifugation (2000 × g, 10 min, 4 °C). The organic layer was removed and combined with the previously-extracted organic layer. The solvent from the combined organic phases was evaporated

under a stream of argon. The tubes were capped and kept overnight at -20°C . The concentrated samples were then resuspended in $52\ \mu\text{L}$ of ice-cold chloroform and divided into two spots of $20\ \mu\text{L}$ each onto $20 \times 20\ \text{cm}$ glass-backed thin layer silica gel chromatography (TLC) plates. The TLC mobile phase consisted of 11:5 isooctane:ethyl acetate saturated with H_2O and acetic acid (Parrish and Nichols, 2006). After the plates were air-dried, the lipids were visualized with iodine vapor. The location of the AEA, 2AG, and ARA spots was identified by comparison with standards (Cayman Lipids). The silica corresponding to the AEA, 2AG, and ARA spots was then scraped off of the TLC plate into scintillation vials and allowed to equilibrate in EcoLite scintillation cocktail (MP Biomedicals) for three days. Radioactivity was then quantified on a Beckman 1801 LS scintillation counter.

For the assay verifying the concentration and time points of ionomycin incubations, RBL-2H3 cells were plated and incubated with $[^3\text{H}]$ AEA as described above. Endocannabinoid biosynthesis was stimulated with 10 nM, 100 nM, 1 μM , 10 μM , or 100 μM ionomycin for 10 min at 37°C . To verify the appropriate time points of ionomycin stimulation, cells were treated with 1 μM ionomycin anywhere between 0.5 min and 10 min at 37°C . In both experiments the reaction buffer was collected, the lipid were extracted and analyzed as described above.

For the assay examining the role of the source of calcium in the biosynthesis of endocannabinoids, RBL-2H3 cells were plated and incubated with $[^3\text{H}]$ AEA as described above. Cells were then treated with 1 μM ionomycin for 10 min or 1 μM thapsigargin (Sigma) for 30 min at 37°C in the presence or absence of calcium. The reaction buffer was collected, the lipids were extracted and analyzed as described above.

High performance liquid chromatography (HPLC) analysis

RBL-2H3 cells were plated at 3×10^5 cells/well seeding density in 6-well culture plates. Twenty four hours after plating, 1 nM $[^3\text{H}]$ AEA was added to the cells. The tritiated species were allowed to metabolize and become incorporated into the membrane for the next 24 hours. Cells were washed and treated with ionomycin to stimulate endocannabinoid synthesis as described above. The reaction buffer was then collected, and the aqueous and organic phases were mixed and separated as described above. The combined organic phases were then evaporated under a stream of argon. Samples were then resuspended in $10\ \mu\text{L}$ of ethanol, and $10\ \mu\text{L}$ of 14.4 μM cold AEA was added to each sample. HPLC analysis was performed using a modification of the published method by Fezza and colleagues (Fezza et al., 2005). Briefly, a Shimadzu Liquid Chromatograph model LC-10AT VP, and a Shimadzu UV detector model C-R5A Chromatopac was used. The separations were carried out on a C18 ($25\ \text{cm} \times 4.6\ \text{mm}$, 5 μm) column (Supelco) with mobile phase composition of methanol:water:acetic acid (85:15:0.1, v:v:v), and flow rate of 0.8 mL/min. Fractions eluting from the HPLC were collected every minute into scintillation vials. UltimaFlo™ AP liquid scintillation cocktail (Perkin-Elmer) was added to the eluted fractions at a 2:1 (v:v) ratio. Radioactivity was then quantified by liquid scintillation counting. The identity of AEA was assessed by comparing the tritium profile in the eluted fractions with the UV detection of the cold standard at 204 nm.

$[^3\text{H}]$ AEA Uptake

RBL-2H3 cells were plated at 1.2×10^5 cells/well seeding density in a 24-well culture plate. Twenty four hours later, cells were washed with KRH buffer (at the indicated pH). Cells were then incubated in KRH buffer for 10 min at 37°C . 1 nM $[^3\text{H}]$ AEA with or without 1 μM ionomycin or 100 μM AM404 were allowed to incubate with the cells for 10 min at 37°C . Cells were washed twice with KRH buffer containing 0.5% fatty acid-free BSA and

once with KRH buffer with no BSA. Microscint-20[®] (Packard) was added to each well and allowed to equilibrate overnight. The accumulated tritium was detected using a Packard Topcount microplate scintillation and luminescence counter. AM404 (100 μ M) was used to define non-specific uptake. The same procedure was used in the experiment designed to evaluate the effect of exogenous calcium on [³H] AEA uptake in RBL-2H3 cells, except in the indicated treatment, KRH buffer with no calcium was used.

Fluorescent detection of SKM 4-45-1 uptake

RBL-2H3 cells were plated at 1.2×10^5 cells/well seeding density on glass coverslips in a 6-well culture plate, that had been coated with poly-D-lysine 1 hour prior to plating. The next day, cells were treated with 25 μ M SKM 4-45-1 (Cayman Lipids) in the presence or absence of 1 μ M ionomycin for 10 min at 37 °C. Cells were then immediately fixed in a 4% paraformaldehyde solution for 30 min at room temperature. Cells were washed twice with phosphate-buffered saline (PBS) for 15 min and twice for 5 min at room temperature. Coverslips were removed from the wells, mounted on slides using ProLong Antifade with DAPI (Molecular Probes), and allowed to dry overnight. The cell images were acquired by oil immersion confocal microscopy at X 60 magnification with a Nikon Diaphot 300 microscope. The Bio-Rad MRC1024 confocal system was used with a krypton (488 nm)/argon (568 nm) laser, a 522-535-nm band-pass filter, and a 588-nm long-pass filter.

For fluorescent detection of SKM 4-45-1 uptake in RBL-2H3 cells using fluorescence spectroscopy, RBL-2H3 cells were plated in 10-cm tissue culture plates. Cells were then washed, and then scraped off the plate in 5 mL KRH buffer. Cells were plated at 1.5×10^4 cells/well seeding density, AM404 (100 μ M) or ionomycin (10 μ M) were immediately added to the suspended cells, and incubated for 10 min at 37 °C. SKM 4-45-1 (25 μ M) was added to the cells for 5 min at 37 °C. Fluorescence intensity was measured using the Fusion[™] α -FP fluorescence spectrometer. Excitation wavelength was set at 485 nm, emission wavelength was set at 535 nm. The instrument settings were as follows: fluorescence bottom read with well read and well repeats were set at 1, lamps intensity was set at 20, gain at 1, photomultiplier tube voltage at 1100 V.

Expression of NAPE PLD in HEK-293 Cells and Cellular Fractionation of HEK-293, RBL-2H3, and CAD Cells

HEK-293 cells were grown to 70 % confluency in 10-cm culture dishes. The cells were transfected with 24 μ g of pcDNA3.1+ NAPE PLD (rat) or pcDNA3.1+ using Lipofectamine 2000 (Invitrogen). The cells were cultured at 37 °C for 48 hours with one change of medium at 4 hours after the start of the transfection. RBL-2H3 and CAD cells were grown in 10-cm culture dishes to 80% confluency. Transfected HEK-293 cells, RBL-2H3 and CAD cells were lysed on ice for 10 min in lysis buffer (2 mM Hepes, 1 mM EDTA, pH 7.4). Cells were scraped off the culture plates and transferred into 2.0 mL flat-bottom microcentrifuge tubes (Avanti). The cell lysates were then subjected to ultracentrifugation at $100,000 \times g$ for 45 min at 4 °C. The supernatants were saved (cytosolic fraction), and the pellets were resuspended in the lysis buffer. The ultracentrifugation step was repeated. The supernatants from this step were discarded. The resulting pellets were resuspended in lysis buffer containing 1% Triton X 100, and incubated on ice for 10 min. The membrane fractions were then separated from the rest of the sample with centrifugation at top speed in an Eppendorf Mini Spin Plus centrifuge (Brinkmann Instruments). The resulting supernatants were saved as the membrane fractions.

Western Blot analysis of NAPE PLD

The membrane and cytosolic fractions were prepared for SDS PAGE by combining the samples with Laemmli buffer in a 1:1 ratio (v:v) (5% bromophenol blue, 5% β -

mercaptoethanol, 62.5 mM Tris-HCl, 20% glycerol, and 2% SDS). Samples were then resolved on a 4–20% polyacrylamide SDS PAGE (BioRad) for 1.5 hours at 105 V using the Mini-Protean 3 system (Bio-Rad). Proteins were then transferred onto a polyvinylidene difluoride membrane using the Bio-Rad Mini Trans-Blot system for 3 hours at 60 V. The membrane was stored in a phosphate-buffered saline (PBS) solution containing 0.1% Tween-20 and 5% dry milk at 4 °C overnight. The presence of NAPE PLD was revealed using the rabbit anti-NAPE PLD polyclonal primary antibody (1:500, Cayman Lipids) and a goat anti-rabbit (1:2000, Bio-Rad) horseradish peroxidase-labeled secondary antibody followed by an exposure with ECL detection reagents (Amersham).

Expression of NAPE PLD and [³H] AEA Recycling and Synthesis in CAD Cells

CAD cells were grown to 70 % confluency in 6-well culture plates, previously coated with poly-D-lysine. The cells were transfected with 4 µg of pcDNA3.1+ NAPE PLD or pcDNA3.1+ using Lipofectamine 2000 (Invitrogen). The cells were cultured at 37 °C for 48 hours with one change of medium at 4 hours after the start of the transfection. 10 nM [³H] AEA was added to the cells 4 hours before the assay. Cells were then washed twice with KRH buffer (pH 7.1) with 0.5% BSA and once with KRH buffer without BSA. Cells were then treated with 1 µM ionomycin for 10 min at 37 °C in order to stimulate endocannabinoid synthesis. The reaction buffer was then collected, prepared, and analyzed by TLC as described above.

Data and Statistical Analysis

The data representing endocannabinoid synthesis and release were normalized to the control (buffer). The counts per minute (CPM) values corresponding to the synthesis and release of endocannabinoids in response to stimuli (ionomycin or thapsigargin) were divided by the average CPM value corresponding to the control, thus yielding a release response as fold over buffer. Data are expressed as mean ± SEM performed in duplicate. A two-tailed student's t test was used to compare two data sets, a one-way ANOVA with Newman-Keul's post-hoc test was performed to compare data sets from more than two sets. $p < 0.05$ was considered statistically significant. GraphPad Prism (v. 3.02) software was used for all statistical analyses.

Results

AEA and 2-AG can be synthesized from exogenous ARA by RBL-2H3 cells

RBL-2H3 cells are a mucosal mast cell line that was successfully used by our lab to study AEA endocytosis (Barsumian et al., 1981; McFarland et al., 2004). To determine whether AEA or 2AG can be formed from exogenously provided ARA, we allowed RBL-2H3 cells to grow in the presence of 1 nM [³H] ARA for 24 hours. AEA and 2AG synthesis and release were stimulated with the treatment of 1 µM ionomycin, an ionophore used to elevate the intracellular calcium concentrations (Liu and Hermann, 1978). The TLC analysis of tritium content in the reaction buffer revealed that RBL-2H3 cells utilized the exogenous ARA to synthesize and release new AEA and 2AG molecules in response to 1 µM ionomycin (Fig. 1). Treatment of the cells with ionomycin resulted in an increased synthesis and release of [³H] AEA compared with the buffer-treated control (Fig. 1A). Pre-treatment of the cells with the AEA uptake inhibitor, AM404 (100 µM), resulted in a decrease of AEA release in response to the stimulation with ionomycin. RBL-2H3 cells also released 2AG and free ARA, similar to AEA (Fig. 1B and C). Again, the synthesis and release of 2AG was attenuated in the presence of AM404. After the pre-treatment with AM404, the release of ARA in response to ionomycin was increased, unlike the response of AEA and 2AG.

The recycling of AEA to form new AEA and 2-AG molecules requires intact membrane microdomains and is blocked by AM404

Our lab had previously shown that AEA metabolites, ARA and ethanolamine, are enriched in the caveolae/lipid raft microdomains of the cell (McFarland et al., 2004). We explored the possibility that these AEA metabolites, ARA and ethanolamine, could be used by the cell to form new endocannabinoid molecules. To examine this hypothesis, we allowed RBL-2H3 cells to accumulate and metabolize [³H] AEA (1 nM) for 24 hours and then stimulated endocannabinoid synthesis and release with the addition of 1 μM ionomycin. The TLC analysis of tritiated products from the reaction buffer revealed that treatment of RBL-2H3 cells with ionomycin resulted in an increased synthesis and release of [³H] AEA compared with the buffer-treated control (Fig. 2A). We verified the results obtained with TLC analysis using HPLC approach. We confirmed that the identity of the peak corresponding to AEA on the UV spectrum corresponded to the [³H] AEA that eluted from the HPLC (Fig. 2A, inset). TLC analysis on cell lysates from cells incubated with [³H] ARA or [³H] AEA confirmed no detectable intact AEA or 2-AG were present in the cells prior to ionomycin stimulation (data not shown). These control experiments suggest that the endocannabinoids detected after ionomycin stimulation represent a newly-synthesized population of AEA and 2-AG and not residual levels remaining from the labeling step.

The synthesis and/or release of AEA was attenuated when the cells were pre-treated with 100 μM AM404 prior to the stimulation with ionomycin (Fig. 2A). The disruption of the lipid raft microdomain organization with nystatin (25 μg/mL)/progesterone (10 μg/mL) treatment (N/P) also resulted in the attenuation of AEA synthesis and/or release when stimulated with ionomycin (Fig. 2A). These results support our hypothesis that AEA metabolites can be recycled to form new AEA molecules, and that this process is dependent on intact lipid raft microdomains. Control cells utilized in the AEA recycling assays were also subjected to lysis and TLC analysis to confirm that no detectable levels of intact AEA remained after the 24 hour incubation (data not shown).

In addition to recycling AEA into new AEA molecules, RBL-2H3 cells recycled AEA-derived ARA into 2-AG and released 2-AG and ARA in response to the treatment with ionomycin (Fig. 2 B and C). Treatment of the cells with 100 μM AM404 resulted in a reduction of 2AG release from RBL-2H3 cells in response to the ionomycin stimulation. The release of ARA in response to ionomycin was unchanged after the pre-treatment with AM404, unlike the response of AEA and 2AG. Treatment of RBL-2H3 cells with nystatin/progesterone (N/P) attenuated 2-AG synthesis and/or release as well as the release of ARA in response to ionomycin.

We verified the time- and dose-dependency of ionomycin stimulation on endocannabinoid biosynthesis. We observed that endocannabinoid biosynthesis is time-dependent with peak production occurring between 7 and 10 minutes (Fig. 3 A and B). These studies also revealed that the maximal endocannabinoid biosynthesis and release was achieved between 100 nM and 1 μM ionomycin (Fig. 3 C and D).

Extracellular calcium is necessary for AEA and 2-AG biosynthesis--release of intracellular calcium stores alone does not promote endocannabinoid biosynthesis

Endocannabinoid biosynthesis is a calcium-dependent process (Piomelli, 2003). We determined how the source of calcium influences biosynthesis of AEA and 2-AG in RBL-2H3 cells. We examined the role of exogenous calcium supplied in the assay buffer, and the role of calcium derived from the depletion of intracellular calcium stores. RBL-2H3 cells were treated with 1 nM [³H] AEA for 24 hours and then endocannabinoid synthesis and release was stimulated with the addition of 1 μM ionomycin or 10 μM thapsigargin, an

agent that raises intracellular calcium concentrations by inhibiting a class of enzymes called sarcoendoplasmic reticulum calcium ATPases. In the presence of extracellular calcium, both ionomycin and thapsigargin stimulated a robust increase in AEA, 2-AG and ARA synthesis and release (Fig. 4). The synthesis and release of AEA and the release of ARA in response to thapsigargin were comparable to that of ionomycin stimulation (Fig. 4A and C). The thapsigargin response for 2-AG synthesis and release was increased compared the ionomycin treatment (Fig. 4B). When the extracellular calcium was removed from the buffer, endocannabinoid synthesis and release was inhibited. The results indicate that the endocannabinoid biosynthetic pathway in RBL-2H3 cells is sensitive to the source of calcium. Extracellular calcium must be present in order to stimulate endocannabinoid synthesis and cannot be substituted with calcium derived only from intracellular calcium stores (i.e., in the case of thapsigargin treatment without extracellular calcium).

Elevation of intracellular calcium reduces the uptake of AEA in RBL-2H3 cells

Our lab has previously demonstrated that AEA uptake is rapid, saturable, temperature-dependent, and most importantly occurs via a non-clathrin mediated endocytic process (McFarland et al., 2008; McFarland et al., 2004). Therefore, we concluded that AEA uptake may take place via caveolae/lipid raft-related endocytosis in RBL-2H3 cells. In the present study, we observed that the synthesis and release of AEA depended on the intact organization of lipid rafts (Fig. 2). If membrane microdomains are involved in the synthesis and release of endocannabinoids, then there must be a cellular mechanism to provide temporal separation between release and uptake events. Because AEA biosynthesis is sensitive to elevated intracellular calcium concentrations, we hypothesized that increasing intracellular calcium concentrations could act as the “switch” to promote AEA biosynthesis and simultaneously suspend the process of uptake. We discovered that [³H] AEA uptake in RBL-2H3 was attenuated in the presence of 1 μM ionomycin as compared with control (Fig. 5A). We were concerned, however, that the decrease in the [³H] AEA uptake was a result of an increase in the synthesis and release of non-tritiated endogenous AEA that was produced in response to the ionomycin treatment. In this case, the newly synthesized and released AEA could be competing for the uptake with [³H] AEA. Therefore, we performed the experiments of [³H] AEA uptake at low pH where AEA synthesis is known to be significantly reduced (Ueda et al., 2001). At pH 7.1, there was a robust increase of AEA synthesis and release upon treatment of the cells with 1 μM ionomycin compared with the buffer-stimulated cells (control) (Fig. 5B). At pH 5.1, however, the synthesis and release of AEA in response to 1 μM ionomycin stimulation was attenuated (Fig. 5B). Even under the conditions where AEA synthesis and release were effectively reduced (pH 5.1), ionomycin treatment inhibited AEA uptake suggesting that new AEA molecules were not responsible for the reduction in transport (Fig. 5C).

The fluorescent derivative of AEA SKM 4-45-1 was used to further explore the impact of intracellular calcium on endocannabinoid uptake. Outside the cell SKM 4-45-1 is non-fluorescent, however once this molecule is taken up by the cells, it undergoes rapid cleavage by nonspecific esterases into AEA and fluorescein (Muthian et al., 2000). SKM 4-45-1 was chosen for this experiment because it has been shown to undergo carrier-mediated uptake via the same mechanism as AEA endocytosis (McFarland et al., 2008; Muthian et al., 2000). We incubated RBL-2H3 with 25 μM SKM 4-45-1 in the presence or absence of 1 μM ionomycin and detected the resulting fluorescence signal in each condition. In the presence of ionomycin, the fluorescence signal was much weaker compared with the signal obtained without the ionomycin treatment (Fig. 5D). This result confirmed that SKM 4-45-1 uptake was reduced by the ionomycin treatment. Furthermore, these results were quantified using fluorescence spectroscopy. RBL-2H3 cells were pre-incubated with AM404 (100 μM) or

ionomycin (10 μ M), and SKM 4-45-1 uptake was evaluated. AM404 blocked SKM 4-45-1 uptake and ionomycin pre-treatment reduced SKM 4-45-1 uptake as well (Fig. 5E).

Once we established that AEA uptake was attenuated in response to increased intracellular calcium concentrations, we determined how exogenous calcium affects AEA uptake. [3 H] AEA uptake in RBL-2H3 was evaluated in the presence and absence of calcium in the uptake buffer. In the absence of calcium, [3 H] AEA uptake was enhanced compared with the results obtained in calcium-containing uptake buffer (Fig. 5F). The finding that calcium attenuated [3 H] AEA uptake in RBL-2H3 further reinforced our hypothesis that cells may utilize calcium as a “switch” between the events of endocannabinoid biosynthesis and uptake.

NAPE PLD may not be involved in the biosynthesis of AEA in RBL-2H3 cells

Previous studies suggested that AEA biosynthesis involves the NAPE PLD-dependent cleavage of *N*-acyl phosphatidylethanolamine (NAPE), the AEA precursor (Okamoto et al., 2004). In this study, we observed that RBL-2H3 cells synthesized and released AEA in response to ionomycin stimulation. Therefore, we further examined the role of NAPE PLD in the formation of AEA in RBL-2H3 cells. Using Western blot analysis, we determined that NAPE PLD expression was not detectable in RBL-2H3 cells (Fig. 6). As a control experiment, we transfected HEK-293 cells with the NAPE PLD cDNA and performed immunoblotting on the lysates of membrane and cytosolic fractions from these transfected cells. Only the HEK-293 cells that had been transfected with the NAPE PLD cDNA exhibited detectable levels of NAPE PLD (Fig. 6).

CAD cells do not recycle AEA to form new 2-AG and AEA molecules

The studies conducted in the RBL-2H3 cell line provided a model for AEA synthesis and release, implicating recycling of AEA metabolites. Next, we attempted to extend the model of AEA recycling into a neuronal-like cell line. The Cath.a catecholaminergic cells possess neuronal properties except they do not have classic neuronal morphology (Suri et al., 1993). Cath.a differentiated (CAD) cells, derived from the Cath.a cell line, were chosen for the next set of experiments in order to validate a neuronal-like cell line to study AEA synthesis. CAD cells do not express the immortalizing oncogene present in Cath.a cells, and display biochemical properties characteristic of neuronal cells (Qi et al., 1997). We have previously used CAD cells to study AEA uptake and observed similar uptake properties to RBL-2H3 cells (McFarland et al., 2008). We used CAD cells to test whether the recycling of AEA is a phenomenon that takes place in neuronal cells similar to AEA recycling in RBL-2H3 cells. CAD cells were incubated in the presence of 10 nM [3 H] AEA for 4 hours. These conditions were optimized for maximum uptake and incorporation of AEA (not shown). The analysis of tritium content in the reaction buffer revealed that treatment of CAD cells with 1 μ M ionomycin did not result in an increase of AEA, 2AG, or ARA release (data not shown) in contrast to the effects observed in RBL-2H3 cells (Fig. 1 and 2).

Endogenous NAPE PLD expression was not detected with immunoblotting analysis in CAD cells (Fig. 6). Therefore, we tested whether CAD cells that expressed exogenous NAPE PLD would recycle [3 H] AEA to form and release new AEA molecules in a similar fashion to RBL-2H3 cells. CAD cells were transfected with the NAPE PLD cDNA, pre-labeled with 10 nM [3 H] AEA for 4 hours, and evaluated for their ability to synthesize and release AEA in response to ionomycin. NAPE PLD expression was confirmed with immunoblotting (data not shown). Treatment of the transfected CAD cells with 1 μ M ionomycin resulted only in a small increase of AEA, but not 2-AG or ARA release compared with the control cells that were transfected with vector (Fig. 7). Thus, wild-type CAD cells do not form and release

AEA, however, CAD cells that express NAPE PLD are capable of a modest synthesis and release of AEA.

Discussion

The process of AEA biosynthesis remains enigmatic despite the abundance of studies performed to characterize the metabolism and signaling of this endocannabinoid. The most widely accepted pathway for the synthesis of AEA involves NAPE PLD, an enzyme that catalyzes the hydrolysis of NAPE to form AEA. In a study by Leung and colleagues (2006), the brain levels of long-chain unsaturated eicosanoids, AEA in particular, remained unchanged in NAPE PLD knock-out mice compared with wild-type animals (Leung et al., 2006). Other labs, however, have shown that NAPE PLD catalyzes the formation of AEA from NAPE *in vitro* (Okamoto et al., 2004). The finding by Leung and colleagues suggests that the formation of AEA *in vivo* may not be necessarily dependent on NAPE PLD despite the ability of this enzyme to form AEA *in vitro* (Leung et al., 2006). In other words, NAPE PLD is able to use NAPE as a substrate to form AEA, however, the native pathway for the formation of AEA may not involve this enzyme *in vivo*. In the present study, we report that NAPE PLD expression in RBL-2H3 cells was not detectable suggesting that NAPE PLD is either not involved with AEA biosynthesis in these cells or low levels of the enzyme are sufficient for biosynthesis. Our inability to detect NAPE PLD expression could reflect a lack of sensitivity in our immunoblots making future studies examining gene expression patterns of this enzyme critical for a full understanding of NAPE PLD's role in endocannabinoid production. Additional pathways for the biosynthesis of AEA have been suggested. Simon and Cravatt reported that AEA formation takes place via α/β hydrolase 4-dependent NAPE hydrolysis followed by a phosphodiesterase cleavage step modulated by glycerophosphodiesterase 1 (Simon and Cravatt, 2006; Simon and Cravatt, 2008). In the future, genetic and pharmacologic approaches should be used to further characterize the roles of α/β hydrolase 4 and glycerophosphodiesterase 1 in the biosynthesis of AEA in RBL-2H3 or other systems.

We report that AEA can be recycled by RBL-2H3 cells to form and release new AEA molecules, 2AG, and release ARA in response to the ionomycin treatment. We also observed that the process of AEA synthesis and release depends on the intact organization of lipid raft/caveolae microdomains. Incubation of the cells with nystatin/progesterone, a treatment known to disrupt lipid rafts (McFarland et al., 2004), resulted in the attenuation of AEA synthesis and release. This result and the fact that AEA metabolites, ARA and ethanolamine, become rapidly enriched in the lipid raft/caveolae fractions of the cell (McFarland et al., 2004) suggest that AEA synthesis and release may, in fact, take place in the lipid raft/caveolae microdomains in RBL-2H3 cells. Although the nystatin/progesterone treatment resulted in a significant reduction of AEA and 2-AG synthesis and/or release in RBL-2H3 cells, the treatment did not completely abolish endocannabinoid biosynthesis. The fact that RBL-2H3 cells were able to produce AEA and 2-AG in response to ionomycin even after the nystatin/progesterone treatment may be explained in two ways. One potential explanation for the above-mentioned phenomenon is that the nystatin/progesterone treatment sequesters only a fraction of the cholesterol stores in the cell. A small portion of intact lipid rafts may remain intact in the nystatin/progesterone-treated cells, therefore, allowing for endocannabinoid biosynthesis to take place. An alternative explanation for the fact that AEA and 2-AG synthesis was not completely abolished in RBL-2H3 cells after nystatin/progesterone treatment is that perhaps not all of the endocannabinoid biosynthesis is dependent on lipid rafts. It is possible that a subset of endocannabinoids is synthesized in the non-lipid raft regions of the cell. Furthermore, we recognize the nonspecific nature of the treatment with nystatin/progesterone, and therefore, suggest that further analytical

approaches will be needed to confirm the role of lipid rafts in endocannabinoid synthesis (Rimmerman et al., 2008).

A reduction in the synthesis and/or release of AEA and 2AG in response to AM404 pre-treatment of RBL-2H3 cells was also observed. AM404 is known to block AEA uptake as well as FAAH (Beltramo et al., 1997). Our results indicate that perhaps in addition to inhibiting FAAH and blocking AEA uptake, AM404 may also prevent AEA and 2AG synthesis and/or release in RBL-2H3 cells. Other groups have also reported that AM404 inhibits AEA release in some cell lines but not others (Hillard and Jarrahian, 2005). The finding that AM404 blocks AEA release in certain systems begs the question as to whether the protein(s) involved with AEA uptake may also be involved in the release of this endocannabinoid.

We discovered that treatment of RBL-2H3 cells with thapsigargin triggered AEA and 2-AG synthesis and release as well as ARA release, in a similar manner to ionomycin. We then investigated if elevating the intracellular calcium concentration by depleting the internal calcium stores alone would trigger endocannabinoid synthesis and release. Our results indicate that depletion of the intracellular calcium stores with thapsigargin without the presence of extracellular calcium was not sufficient for endocannabinoid synthesis and release. Liu and colleagues have shown that depletion of internal calcium stores with thapsigargin activates cation channels in the plasma membranes of RBL-2H3 cells (Liu et al., 2004). In our experiments, endocannabinoid biosynthesis could only be stimulated when extracellular calcium was supplied in the buffer. Therefore, a possible explanation of the endocannabinoid biosynthesis mechanism response in RBL-2H3 cells in response to thapsigargin may involve store-operated Ca^{2+} entry (SOCE). Calcium entry that is modulated by depletion of intracellular calcium stores (primarily from the endoplasmic reticulum) is called SOCE and is mediated via the activation of specific plasma membrane channels, termed store-operated calcium (SOC) channels (Hewavitharana et al., 2007). Additional experiments performed with blockers of voltage-gated calcium channels (L-type channels, nifedipine; N-type channels, ω -conotoxin GVIA; R-type channels, SNX482) attempting to identify the channel involved with AEA biosynthesis. These compounds failed to reduce thapsigargin-induced synthesis of AEA or 2-AG (data not shown) suggesting that other channels such as those involved with SOCE (i.e., TRPC channels) may be mediating the required calcium influx. Pani and colleagues showed that in HSG and HEK-2H9 cells the molecular organization of SOCE is modulated by lipid rafts microdomains (Pani et al., 2008). Whether or not lipid raft microdomains regulate SOCE in RBL-2H3 cells remains unknown. The subject of future investigations should focus on characterizing the potential role of lipid rafts in modulating SOCE, and the role of SOCE in the biosynthesis of endocannabinoids in RBL-2H3 cells.

We explored the possibility that the cell may use calcium as a “switch” between the process of AEA endocytosis and biosynthesis. We have shown that AEA biosynthesis depends on the influx of calcium and requires intact organization of lipid rafts. Our lab has previously shown that the uptake of AEA takes place via caveolae-related endocytosis (McFarland et al., 2008; McFarland et al., 2004). Therefore, we explored the question as to how two different processes, endocytosis and release, may take place in the same microdomain of the cell. We hypothesized that the cells use intracellular calcium to act as the “switch” to activate synthesis and simultaneously suspend uptake of AEA. In other words, once the demand for the synthesis of AEA is triggered by an influx of calcium, the process of endocytosis is inhibited. We discovered that in the presence of ionomycin, the uptake of [^3H] AEA was attenuated compared with the buffer-treated control. We also tested whether the inhibition of [^3H] AEA uptake was a result of the release of endogenous, non-tritiated AEA that was competing with [^3H] AEA. At pH 5.1, there was a significant decrease in the

uptake of [^3H] AEA when the cells were treated with ionomycin, a result comparable to that obtained at pH 7.1. The synthesis of AEA, however, was greatly reduced at pH 5.1 compared with the results acquired at pH 7.1. Therefore, we concluded that the endogenous newly-synthesized AEA was not competing with [^3H] AEA for uptake, but rather that the influx of calcium in response to the ionomycin treatment attenuated [^3H] AEA uptake. Furthermore, the increase in intracellular calcium not only caused a decrease in the uptake of AEA, but also the presence of extracellular calcium reduced the uptake of AEA as well. The molecular pathway involving calcium that is capable of regulating AEA uptake remains unknown and should, therefore, be the focus of future studies.

Our study primarily examined the patterns of endocannabinoid biosynthesis and release in RBL-2H3 cells. We attempted to address the significance of these patterns in a neuronal system. We chose to use CAD cells as a neuronal model to test whether the recycling of AEA is a generally observed phenomenon. We had previously used CAD cells to study endocannabinoid uptake and showed that these cells express an endocannabinoid phenotype including the expression of FAAH (McFarland et al., 2008). Our results indicate that CAD cells were not able to recycle AEA because 2-AG and AEA synthesis could not be achieved after stimulation with ionomycin. Overexpression of NAPE PLD in CAD cells resulted in a modest increase of AEA synthesis and release in response to ionomycin indicating that under specific conditions, NAPE PLD may catalyze the formation of AEA.

The recycling and biosynthesis of endocannabinoids appear to be cell model-specific processes. Our studies suggest that in RBL-2H3 cells, trafficking pathways exist for the effective handling of AEA metabolites such that the ARA and ethanolamine can be recycled to form new endocannabinoid molecules. Based on the present data as well as our previous work on the role of caveolae in AEA endocytosis, we propose that these membrane microdomains serve as critical scaffolds for sequestering endocannabinoid metabolites and precursors as well as possibly biosynthetic machinery. Future studies should focus on identifying the protein(s) involved with AEA and 2-AG biosynthesis and determining if these proteins are also enriched in the lipid raft/caveolae microdomains. Furthermore, future studies of endocannabinoid biosynthesis should be extended into primary neuronal or astrocytic cultures to establish the ability of cells to recycle efficiently the arachidonate backbone of AEA into new endocannabinoid molecules.

Acknowledgments

This work was supported by the National Institutes of Health grant R21 DA018112. We thank Dr. Jason Parrish for help with TLC analysis and Dr. Gary Carlson and Nancy Mantick for help with HPLC. A special thanks to David Allen and Jennie Sturgis for help with image preparation.

abbreviations used in text

2-AG	2-arachidonyl glycerol
ARA	arachidonic acid
AEA	arachidonyl ethanolamine (anandamide)
BSA	bovine serum albumin
Δ^9-THC	delta-9-tetrahydrocannabinol
CPM	counts per minute
FAAH	fatty acid amide hydrolase
HPLC	high performance liquid chromatography

KRH	Kreb-Ringer Hepes
NAE	<i>N</i> -acylethanolamine
NAPE PLD	<i>N</i> -acyl phosphatidylethanolamine phospholipase D
PBS	phosphate-buffered saline
TLC	thin layer chromatography
SOCE	store-operated calcium entry

References

- Barsumian EL, Isersky C, Petrino MG, Siraganian RP. IgE-induced histamine release from rat basophilic leukemia cell lines: isolation of releasing and nonreleasing clones. *Eur J Immunol.* 1981; 11:317–323. [PubMed: 6166481]
- Beltramo M, Stella N, Calignano A, Lin SY, Makriyannis A, Piomelli D. Functional role of high-affinity anandamide transport, as revealed by selective inhibition. *Science.* 1997; 277:1094–1097. [PubMed: 9262477]
- Bisogno T, Howell F, Williams G, Minassi A, Cascio MG, Ligresti A, Matias I, Schiano-Moriello A, Paul P, Williams EJ, Gangadharan U, Hobbs C, Di Marzo V, Doherty P. Cloning of the first sn1-DAG lipases points to the spatial and temporal regulation of endocannabinoid signaling in the brain. *J Cell Biol.* 2003; 163:463–468. [PubMed: 14610053]
- Chevalere V, Takahashi KA, Castillo PE. Endocannabinoid-mediated synaptic plasticity in the CNS. *Annu Rev Neurosci.* 2006; 29:37–76. [PubMed: 16776579]
- Childers SR, Breivogel CS. Cannabis and endogenous cannabinoid systems. *Drug Alcohol Depend.* 1998; 51:173–187. [PubMed: 9716939]
- Cravatt BF, Lichtman AH. Fatty acid amide hydrolase: an emerging therapeutic target in the endocannabinoid system. *Curr Opin Chem Biol.* 2003; 7:469–475. [PubMed: 12941421]
- Deutsch DG, Chin SA. Enzymatic synthesis and degradation of anandamide, a cannabinoid receptor agonist. *Biochem Pharmacol.* 1993; 46:791–796. [PubMed: 8373432]
- Di Carlo G, Izzo AA. Cannabinoids for gastrointestinal diseases: potential therapeutic applications. *Expert Opin Investig Drugs.* 2003; 12:39–49.
- Di Marzo V. ‘Endocannabinoids’ and other fatty acid derivatives with cannabimimetic properties: biochemistry and possible physiopathological relevance. *Biochim Biophys Acta.* 1998; 1392:153–175. [PubMed: 9630590]
- Di Marzo V, Bisogno T, Sugiura T, Melck D, De Petrocellis L. The novel endogenous cannabinoid 2-arachidonoylglycerol is inactivated by neuronal- and basophil-like cells: connections with anandamide. *Biochem J.* 1998; 331:15–19. [PubMed: 9512456]
- Fezza F, Gasperi V, Mazzei C, Maccarrone M. Radiochromatographic assay of *N*-acyl-phosphatidylethanolamine-specific phospholipase D activity. *Anal Biochem.* 2005; 339:113–120. [PubMed: 15766717]
- Goparaju SK, Ueda N, Yamaguchi H, Yamamoto S. Anandamide amidohydrolase reacting with 2-arachidonoylglycerol, another cannabinoid receptor ligand. *FEBS Lett.* 1998; 422:69–73. [PubMed: 9475172]
- Guzmán M. Cannabinoids: potential anticancer agents. *Nat Rev Cancer.* 2003; 3:745–755. [PubMed: 14570037]
- Habayeb OM, Bell SC, Konje JC. Endogenous cannabinoids: metabolism and their role in reproduction. *Life Sci.* 2002; 70:1963–1977. [PubMed: 12148689]
- Hewavitharana T, Deng X, Soboloff J, Gill DL. Role of STIM and Orai proteins in the store-operated calcium signaling pathway. *Cell Calcium.* 2007; 42:173–182. [PubMed: 17602740]
- Hillard CJ, Jarrarian A. Accumulation of anandamide: Evidence for cellular diversity. *Neuropharmacology.* 2005; 48:1072–1078. [PubMed: 15910883]

- Karsak M, Gaffal E, Date R, Wang-Eckhardt L, Rehnelt J, Petrosino S, Starowicz K, Steuder R, Schlicker E, Cravatt BF, Mechoulam R, Buettner R, Werner S, Di Marzo V, Tüting T, Zimmer A. Attenuation of allergic contact dermatitis through the endocannabinoid system. *Science*. 2007; 316:1494–1497. [PubMed: 17556587]
- Lambert DM, Fowler CJ. The endocannabinoid system: drug targets, lead compounds, and potential therapeutic applications. *J Med Chem*. 2005; 48:5059–5087. [PubMed: 16078824]
- Leung D, Saghatelian A, Simon GM, Cravatt BF. Inactivation of N-acyl phosphatidylethanolamine phospholipase D reveals multiple mechanisms for the biosynthesis of endocannabinoids. *Biochemistry*. 2006; 45:4720–4726. [PubMed: 16605240]
- Liu C, Hermann TE. Characterization of ionomycin as a calcium ionophore. *J Biol Chem*. 1978; 253:5892–5894. [PubMed: 28319]
- Liu X, Groschner K, Ambudkar IS. Distinct Ca(2+)-permeable cation currents are activated by internal Ca(2+)-store depletion in RBL-2H3 cells and human salivary gland cells, HSG and HSY. *J Membr Biol*. 2004; 200:93–104. [PubMed: 15520907]
- London E, Brown DA. Insolubility of lipids in triton X-100: physical origin and relationship to sphingolipid/cholesterol membrane domains (rafts). *Biochim Biophys Acta*. 2000; 1508:182–195. [PubMed: 11090825]
- Matsuda LA, Lolait SJ, Brownstein MJ, Young AC, Bonner TI. Structure of a cannabinoid receptor and functional expression of the cloned cDNA. *Nature*. 1990; 346:561–564. [PubMed: 2165569]
- McFarland MJ, Bardell TK, Yates ML, Placzek EA, Barker EL. RNAi-Mediated Knockdown of Dynamin 2 Reduces Endocannabinoid Uptake Into Neuronal dCAD Cells. *Mol Pharmacol*. 2008; 74:101–108. [PubMed: 18436710]
- McFarland MJ, Porter AC, Rakhshan FR, Rawat DS, Gibbs RA, Barker EL. A role for caveolae/lipid rafts in the uptake and recycling of the endogenous cannabinoid anandamide. *J Biol Chem*. 2004; 279:41991–41997. [PubMed: 15292270]
- Munro S, Thomas KL, Abu-Shaar M. Molecular characterization of a peripheral receptor for cannabinoids. *Nature*. 1993; 365:61–65. [PubMed: 7689702]
- Muthian S, Nithipatikom K, Campbell WB, Hillard CJ. Synthesis and characterization of a fluorescent substrate for the N-arachidonylethanolamine (anandamide) transmembrane carrier. *J Pharmacol Exp Ther*. 2000; 293:289–295. [PubMed: 10734181]
- Okamoto Y, Morishita J, Tsuboi K, Tonai T, Ueda N. Molecular characterization of a phospholipase D generating anandamide and its congeners. *J Biol Chem*. 2004; 279:5298–5305. [PubMed: 14634025]
- Pani B, Ong HL, Liu X, Rauser K, Ambudkar IS, Singh BB. Lipid rafts determine clustering of STIM1 in ER-plasma membrane junctions and regulation of SOCE. *J Biol Chem*. 2008; 283:17333–17340. [PubMed: 18430726]
- Parolaro D, Massi P, Rubino T, Monti E. Endocannabinoids in the immune system and cancer. *Prostaglandins Leukot Essent Fatty Acids*. 2002; 66:319–332. [PubMed: 12052046]
- Parrish JC, Nichols DE. Serotonin 5-HT(2A) receptor activation induces 2-arachidonoylglycerol release through a phospholipase c-dependent mechanism. *J Neurochem*. 2006; 99:1164–1175. [PubMed: 17010161]
- Pertwee RG. Cannabinoid receptors and pain. *Prog Neurobiol*. 2001; 63:569–611. [PubMed: 11164622]
- Pike LJ, Han X, Chung KN, Gross RW. Lipid rafts are enriched in arachidonic acid and plasmenylethanolamine and their composition is independent of caveolin-1 expression: a quantitative electrospray ionization/mass spectrometric analysis. *Biochemistry*. 2002; 41:2075–2088. [PubMed: 11827555]
- Piomelli D. The molecular logic of endocannabinoid signalling. *Nat Rev Neurosci*. 2003; 4:873–884. [PubMed: 14595399]
- Qi Y, Wang JK, McMillian M, Chikaraishi DM. Characterization of a CNS cell line, CAD, in which morphological differentiation is initiated by serum deprivation. *J Neurosci*. 1997; 17:1217–1225. [PubMed: 9006967]
- Razani B, Woodman SE, Lisanti MP. Caveolae: from cell biology to animal physiology. *Pharmacol Rev*. 2002; 54:431–467. [PubMed: 12223531]

- Rimmerman N, Hughes HV, Bradshaw HB, Pazos MX, Mackie K, Prieto AL, Walker JM. Compartmentalization of endocannabinoids into lipid rafts in a dorsal root ganglion cell line. *Br J Pharmacol.* 2008; 153:380–389. [PubMed: 17965731]
- Rothberg KG, Heuser JE, Donzell WC, Ying YS, Glenney JR, Anderson RG. Caveolin, a protein component of caveolae membrane coats. *Cell.* 1992; 68:673–682. [PubMed: 1739974]
- Simon GM, Cravatt BF. Endocannabinoid biosynthesis proceeding through glycerophospho-N-acyl ethanolamine and a role for alpha/beta-hydrolase 4 in this pathway. *J Biol Chem.* 2006; 281:26465–26472. [PubMed: 16818490]
- Simon GM, Cravatt BF. Anandamide biosynthesis catalyzed by the phosphodiesterase GDE1 and detection of glycerophospho-N-acyl ethanolamine precursors in mouse brain. *J Biol Chem.* 2008; 283:9341–9349. [PubMed: 18227059]
- Smart D, Gunthorpe MJ, Jerman JC, Nasir S, Gray J, Muir AI, Chambers JK, Randall AD, Davis JB. The endogenous lipid anandamide is a full agonist at the human vanilloid receptor (hVR1). *Br J Pharmacol.* 2000; 129:227–230. [PubMed: 10694225]
- Smart EJ, Ying Y, Donzell WC, Anderson RG. A role for caveolin in transport of cholesterol from endoplasmic reticulum to plasma membrane. *J Biol Chem.* 1996; 271:29427–29435. [PubMed: 8910609]
- Suri C, Fung BP, Tischler AS, Chikaraishi DM. Catecholaminergic cell lines from the brain and adrenal glands of tyrosine hydroxylase-SV40 T antigen transgenic mice. *J Neurosci.* 1993; 13:1280–1291. [PubMed: 7680068]
- Tramèr MR, Carroll D, Campbell FA, Reynolds DJ, Moore RA, McQuay HJ. Cannabinoids for control of chemotherapy induced nausea and vomiting: quantitative systematic review. *BMJ.* 2001; 323:16–21. [PubMed: 11440936]
- Ueda N, Liu Q, Yamanaka K. Marked activation of the N-acylphosphatidylethanolamine-hydrolyzing phosphodiesterase by divalent cations. *Biochim Biophys Acta.* 2001; 1532:121–127. [PubMed: 11420181]
- Watson SJ, Benson JAJ, Joy JE. Marijuana and medicine: assessing the science base: a summary of the 1999 Institute of Medicine report. *Arch Gen Psychiatry.* 2000; 57:547–552. [PubMed: 10839332]
- Zygmunt PM, Petersson J, Andersson DA, Chuang H, Sjørgård M, Di Marzo V, Julius D, Högestätt ED. Vanilloid receptors on sensory nerves mediate the vasodilator action of anandamide. *Nature.* 1999; 400:452–457. [PubMed: 10440374]

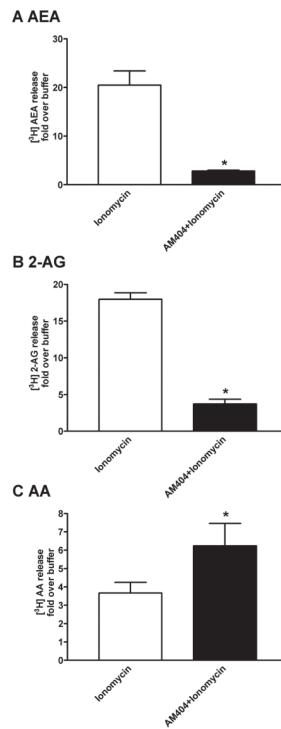


Figure 1. Endocannabinoids can be synthesized from exogenous ARA by RBL-2H3 cells
 RBL-2H3 cells were incubated with 1 nM [³H] ARA for 24 hours. Cells were washed and pre-treated with 100 μM AM404 for 10 min at 37 °C or KRH buffer without AM404. Cells were then treated either with buffer or 1 μM ionomycin for 10 min at 37 °C in order to stimulate AEA (A) and 2AG (B) synthesis and release, or ARA (C) release. The reaction buffer was collected, and the lipids were separated and analyzed as described in Materials and Methods. One-way ANOVA with Newman-Keul's post-hoc test was performed for statistical analysis. * p<0.05, ionomycin vs. AM404+ionomycin. Data represent mean ± SEM from three separate experiments performed in duplicate. CPM values (means ± SEM) for [³H] AEA synthesis and release were: buffer = 87 ± 23; ionomycin = 1788 ± 736; and AM404+ionomycin = 243 ± 61. For [³H] 2-AG synthesis and release: buffer = 32 ± 6; ionomycin = 585 ± 95; and AM404+ionomycin = 138 ± 54. For [³H] ARA release: buffer = 49 ± 10; ionomycin = 166 ± 75; and AM404+ionomycin = 306 ± 143.

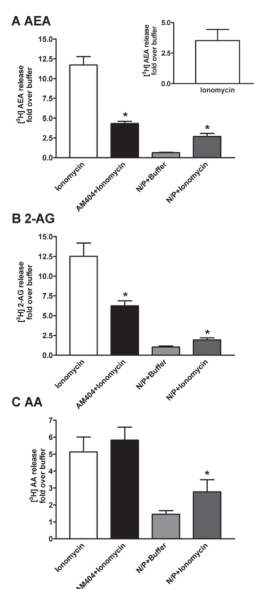


Figure 2. The recycling of AEA to form new AEA and 2-AG molecules requires intact lipid rafts and is blocked with AM404

RBL-2H3 cells were incubated with 1 nM [^3H] AEA for 24 hours. Cells were washed and then treated with nystatin (25 $\mu\text{g}/\text{mL}$)/progesterone (10 $\mu\text{g}/\text{mL}$) (N/P) or KRH buffer without nystatin and progesterone for 30 min at 37 $^{\circ}\text{C}$. One of the indicated treatment conditions included a 100 μM AM404 treatment (10 min at 37 $^{\circ}\text{C}$). Cells were then treated either with buffer or 1 μM ionomycin for 10 min at 37 $^{\circ}\text{C}$ in order to stimulate AEA (A) and 2AG (B) synthesis and release, or ARA (C) release. The extracellular reaction buffer was collected, and the lipids were separated and analyzed as described in Materials and Methods. The results obtained with TLC analysis were confirmed using an HPLC method. The identity of the peak corresponding to AEA on the UV spectrum corresponded to the [^3H] AEA that eluted from the HPLC (inset). One-way ANOVA with Newman-Keul's post-hoc test was performed for statistical analysis. * $p < 0.05$, ionomycin vs. AM404+ionomycin or ionomycin vs. N/P+ionomycin. Data represent mean \pm SEM from three separate experiments performed in duplicate. CPM values (means \pm SEM) for [^3H] AEA synthesis and release were: buffer = 60 ± 18 ; ionomycin = 689 ± 157 ; AM404+ionomycin = 253 ± 38 ; N/P+buffer = 37 ± 5 ; and N/P+ionomycin = 152 ± 35 . For [^3H] 2-AG synthesis and release: buffer = 31 ± 5 ; ionomycin = 395 ± 170 ; AM404+ionomycin = 195 ± 65 ; N/P+buffer = 31 ± 7 ; and N/P+ionomycin = 58 ± 13 . For [^3H] ARA release: buffer = 56 ± 15 ; ionomycin = 308 ± 186 ; AM404+ionomycin = 345 ± 178 ; N/P+buffer = 86 ± 46 ; and N/P+ionomycin = 174 ± 147 .

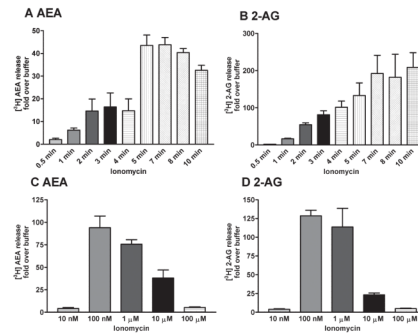


Figure 3. Ionomycin-stimulated endocannabinoid biosynthesis is time- and dose-dependent
 RBL-2H3 cells were incubated with 1 nM [³H] AEA for 24 hours. To verify the appropriate time points of ionomycin stimulation, cells were treated with 1 μM ionomycin at increasing time points from 0.5 min to 10 min at 37 °C to trigger the synthesis and release of AEA (A) and 2-AG (B). Cells were washed and treated with 10 nM, 100 nM, 1 μM, 10 μM, or 100 μM ionomycin for 10 min at 37 °C to stimulate AEA (C) and 2-AG (D) synthesis and release. In both experiments the reaction buffer was collected, the lipids were extracted and analyzed as described in Materials and Methods. Data represent mean ± SEM from two separate experiments performed in duplicate. In panels A and B, the CPM values (mean ± SEM) for [³H] AEA synthesis and release were: buffer = 18 ± 1 and ionomycin stimulation for 10 min = 2775 ± 2611; [³H] 2-AG synthesis and release were: buffer = 18 ± 8 and ionomycin stimulation for 10 min = 1462 ± 905. In panels C and D, the CPM values (mean ± SEM) for [³H] AEA synthesis and release were: buffer = 31 ± 11, 10 nM = 117 ± 34, 100 nM = 2760 ± 683, 1 μM = 2246 ± 515, 10 μM = 1040 ± 214, 100 μM = 166 ± 95; for [³H] 2-AG synthesis and release CPM values were buffer = 14 ± 2, 10 nM = 55 ± 25, 100 nM = 1755 ± 119, 1 μM = 1517 ± 537, 10 μM = 315 ± 34, 100 μM = 68 ± 26.

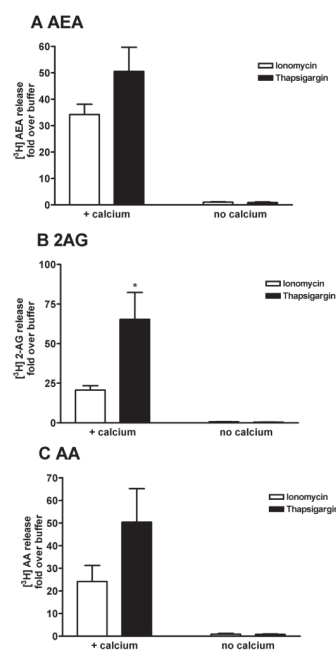


Figure 4. Extracellular calcium is necessary for AEA and 2-AG biosynthesis--release of intracellular calcium stores alone does not promote endocannabinoid biosynthesis
 RBL-2H3 cells were incubated with 1 nM [^3H] AEA for 24 hours. Cells were washed and then treated either with buffer, 1 μM ionomycin for 10 min or 10 μM thapsigargin at 37 $^{\circ}\text{C}$ in the presence or absence of calcium in order to stimulate AEA (A) and 2AG (B) synthesis and release, or ARA (C) release. The extracellular reaction buffer was collected, and the lipids were separated and analyzed as described in Materials and Methods. One-way ANOVA with Newman-Keul's post-hoc test was performed for statistical analysis. * $p < 0.05$, ionomycin vs. thapsigargin. Data represent mean \pm SEM from three separate experiments performed in duplicate. CPM values (means \pm SEM) for [^3H] AEA synthesis and release in the presence of calcium were: buffer = 45 ± 18 ; ionomycin = 1465 ± 200 ; and thapsigargin = 2397 ± 1515 . In the absence of calcium values were: buffer = 57 ± 25 ; ionomycin = 61 ± 90 ; and thapsigargin = 49 ± 24 . For [^3H] 2-AG synthesis and release: buffer = 29 ± 21 ; ionomycin = 521 ± 191 ; and thapsigargin = 1619 ± 787 . [^3H] 2-AG synthesis in the absence of calcium were: buffer = 59 ± 42 ; ionomycin = 38 ± 34 ; and thapsigargin = 19 ± 10 . For [^3H] ARA release: buffer = 49 ± 28 ; ionomycin = 871 ± 698 ; and thapsigargin = 1665 ± 1247 . In the absence of calcium values were: buffer = 116 ± 138 ; ionomycin = 56 ± 41 ; and thapsigargin = 45 ± 15 .

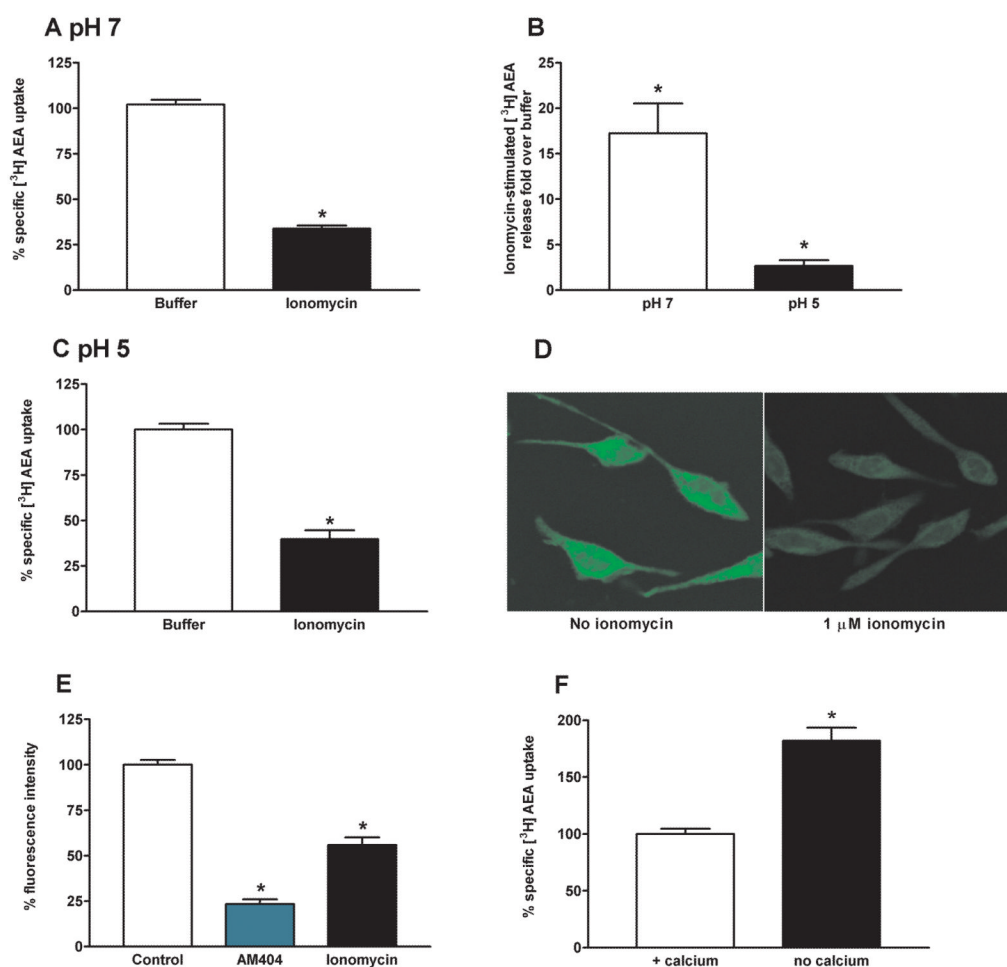


Figure 5. Elevation of intracellular calcium reduces AEA uptake in RBL-2H3 cells

RBL-2H3 cells were incubated with 1 nM [^3H] AEA in the presence or absence of 1 μM ionomycin for 10 min at 37 $^{\circ}\text{C}$ at pH 7.1 (A) or 5.1 (C). The assay was performed in the presence or absence of AM404 (100 μM) in order to define nonspecific uptake. B) Cells were incubated with 1 nM [^3H] AEA for 24 hours, and AEA synthesis was evaluated at pH 5.1 or 7.1. D) SKM 4-45-1 uptake in RBL-2H3 cells was investigated in the presence or absence of 1 μM ionomycin and detected with fluorescence microscopy. E) RBL-2H3 cells were incubated with AM404 (100 μM) or ionomycin (10 μM) for 10 min prior to adding SKM 4-45-1 (25 μM) at 37 $^{\circ}\text{C}$. Fluorescence intensity was measured on the FusionTM α -FP fluorescence spectrometer. Excitation wavelength was set at 485 nm, emission wavelength was set at 535 nm. The instrument settings were as follows: fluorescence bottom read with well read and well repeats were set at 1, lamps intensity was set at 20, gain at 1, photomultiplier tube voltage at 1100 V. F) RBL-2H3 cells were incubated with 1 nM [^3H] AEA in the presence or absence calcium in the buffer for 10 min at 37 $^{\circ}\text{C}$ at pH 7.1. The assay was performed in the presence or absence of AM404 (100 μM) in order to define nonspecific uptake. In panels A-C a two-tailed paired t-test was performed for statistical analysis, * $p < 0.05$. In panel E a one-way ANOVA with Newman-Keul's post-hoc test was performed for statistical analysis, * $p < 0.05$. In panel F a two-tailed paired t-test was performed for statistical analysis, * $p < 0.05$. Data represent mean \pm SEM from three separate experiments performed in duplicate. Mean \pm SEM CPM values corresponding to the specific [^3H] AEA uptake were: buffer = 5008 \pm 764 and ionomycin = 2232 \pm 564. CPM values

corresponding to the synthesis of [^3H] AEA at pH 7 were: buffer = 43 ± 9 and ionomycin = 964 ± 406 ; and at pH 5 were: buffer = 39 ± 8 and ionomycin = 123 ± 79 . The arbitrary fluorescence units corresponding to the total uptake of SKM 4-45-1 were 18850 ± 4178 , AM404 = 9890 ± 2001 , and ionomycin = 15973 ± 3625 .



Figure 6. NAPE PLD is not detectable in RBL-2H3 cells or CAD cells

HEK-293 cells, transfected either with pcDNA3.1+ NAPE PLD or vector pcDNA3.1+, and RBL-2H3 cells were lysed on ice for 10 min in lysis buffer. The whole cell lysates were then subjected to separation into the cytosolic and membrane fractions as described in Materials and Methods. The samples were then resolved on SDS PAGE and transferred onto a polyvinylidene difluoride membrane. The presence of NAPE PLD (46 kDa) was revealed using the rabbit anti-NAPE PLD polyclonal primary antibody (1:500, Cayman Lipids) and a goat anti-rabbit (1:2000), horseradish peroxidase-labeled secondary antibody followed by an exposure with ECL detection reagents. Data are representative of three separate experiments.

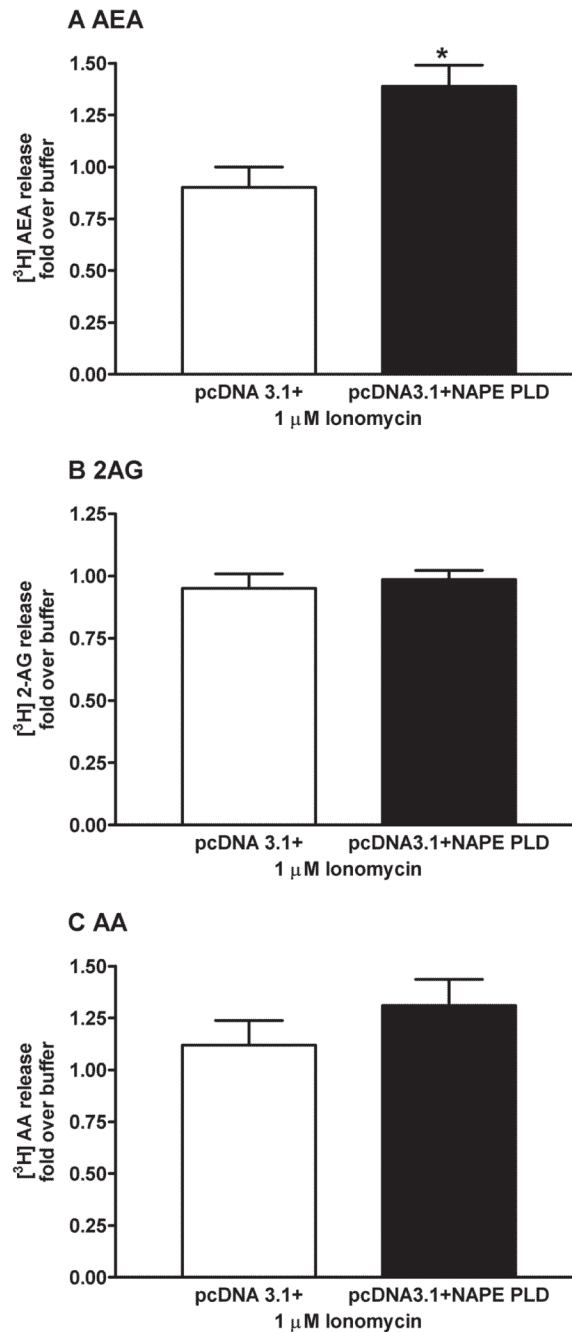


Figure 7. CAD cells transfected with NAPE PLD cDNA recycle AEA to form new AEA molecules

CAD cells were transfected with NAPE PLD pcDNA3.1+ (4 μ g) or pcDNA3.1+ (4 μ g) for 48 hours. CAD cells were then incubated with 10 nM [³H] AEA for 4 hours at 37 °C. Cells were treated with buffer or 1 μ M ionomycin for 10 min at 37 °C in order to stimulate AEA (A) and 2AG (B) synthesis and release, or ARA (C) release. The reaction buffer was collected, the lipids were extracted and analyzed as described in Materials and Methods. A two-tailed paired t-test was performed for statistical analysis, * $p < 0.05$. Data represent mean \pm SEM from three separate experiments performed in duplicate. CPM values (means \pm SEM) for [³H] AEA synthesis and release in CAD cells transfected with pcDNA 3.1+ were:

buffer = 107 ± 36 and ionomycin = 96 ± 36 . Values for pcDNA 3.1+ NAPE PLD were: buffer = 92 ± 24 and ionomycin = 132 ± 52 . For [^3H] 2-AG synthesis and release in CAD cells transfected with pcDNA 3.1+ values were: buffer = 41 ± 19 and ionomycin = 32 ± 12 . Values for pcDNA 3.1+ NAPE PLD were: buffer = 39 ± 16 and ionomycin = 35 ± 13 . For [^3H] ARA release in CAD cells transfected with pcDNA 3.1+ values were: buffer = 152 ± 90 and ionomycin = 152 ± 55 . Values for pcDNA 3.1+ NAPE PLD were: buffer = 128 ± 57 and ionomycin = 180 ± 113 .